Investigation of Dynamics of Poly(dimethylsilane) in the Mesophase by Solid-State ^{29}Si NMR: Evidence for Rotator Phase

Hironori Kaji* and Fumitaka Horii

Institute for Chemical Research, Kyoto University, Uji, Kyoto 611-0011, Japan

Received April 3, 2007; Revised Manuscript Received May 23, 2007

ABSTRACT: The dynamics of poly(dimethylsilane) (PDMS) in the mesophase was investigated by DSC and ^{29}Si solid-state NMR. A solid−solid transition is observed at 166 °C based on DSC measurements. Below the transition temperature, typical chemical shift anisotropy (CSA) spectra are obtained by the ^{29}Si solid-state NMR with cross-polarization (CP) preparation for the static PDMS sample. In contrast, the intensities at the isotropic chemical shift are suppressed for the CSA spectra above the transition temperature. The intensity attenuation, termed "magic angle hole", in the CSA spectra is theoretically derived for uniaxially rotating solids. Therefore, it was found that PDMS undergoes a uniaxial rotation motion above the transition temperature. Theoretically, both the direct polarization (DP) experiments without the CP process and ultraslow magic angle spinning (MAS) experiments retrieve standard CSA line shapes. Our DP and ultraslow MAS experiments confirm the theoretical consideration. The retrieved CSA spectra have axially symmetric line shapes, which also confirm the above uniaxial dynamics. On the basis of the solid-state NMR, we clearly show that the solid−solid transition at 166 °C is a rigid monoclinic−mobile rotator phase transition.

Introduction

The characterization of the structure and dynamics of materials is an important fundamental to understand their properties. For oligomers and polymers, intermediate states, called "mesophases", often appear between the crystalline and liquid (or amorphous) states. As reviewed by Wunderlich et al.,[1] Ungar,[2] and Auriemma et al.,[3] mesophases can be categorized into differently defined several types of phases. Roughly speaking, mesophases are disordered and highly mobile crystalline phases (or ordered and less-mobile liquid phases). The dynamics in the mesophases is closely related to important problems in oligomer and polymer science, such as chain folding[4−9] and (ultra)drawability.[10−16] Therefore, a tremendous amount of research has been carried out for oligomers and polymers with C−C backbones.

In contrast, the oligomers and polymers with Si−Si backbones are less characterized; in particular, their dynamics is less studied. Poly(dimethylsilane) (PDMS) is the simplest polysilane, which has two methyl groups in one main chain Si, $(-Si(CH_3)_2-)_n$. The conformation of the backbone Si−Si bonds, which is directly related to the σ-conjugated states, was studied by electron diffraction measurements by Lovinger et al.[17] and was determined to be all-trans or at least nearly all-trans at room temperature. With increasing temperature, an endothermic peak corresponding to a solid−solid transition was observed at about 160 °C by DSC measurements.[17,18] The X-ray and electron diffraction measurements[17] show a monoclinic packing with $a = 1.218$ nm, $b = 0.800$ nm, c (chain axis) $= 0.388$ nm, and $\gamma = 91°$ below the transition and metrically hexagonal packing with the lattice of $a = (b =) 0.779$ nm above the transition. Lovinger et al. considered three possibilities for the change in the intermolecular packing: the change in the molecular conformation to a disordered or helical conformation, etc., that of packing by transitioning into the rotator phase, etc., and that into a liquid crystalline phase such as the nematic phase. However, the UV and electron diffraction experiments show the preservation of the nearly trans conformation. The other two possibilities are also denied by the electron diffraction experiments. Varma-Nair and Wunderlich et al., who also observed the DSC endothermic peak,[18] assumed that no significant mobility change occurs below and above the transition. Therefore, the origin of the solid−solid transition has not been solved.

In this study, the dynamics of PDMS in the mesophase was studied by ^{29}Si solid-state NMR. The temperature changes of the ^{29}Si chemical shift anisotropy (CSA) powder patterns clearly showed the experimental evidence that PDMS is in the rotator phase above 166 °C, which provides new additional insight into the dynamics of the PDMS.

Experimental Section

PDMS powders, purchased from Wako Pure Chemical Industries, Ltd., were used after annealing at 240 °C for 5 min under N_2 gas. The solid-state ^{29}Si NMR measurements were conducted using a Chemagnetics CMX-400 spectrometer operating with a static magnetic field of 9.4 T (^{29}Si frequency of 79.22 MHz). A double-resonance probe with a 7.5 mm magic angle spinning (MAS) probehead was used. Three types of ^{29}Si CSA experiments were carried out in this study. The standard CSA measurements with CP preparation (CP/CSA measurements) were carried out for the static sample (without MAS) under the condition of the ^{1}H and ^{29}Si field strengths $\gamma B_1/2\pi$ of 50.0 kHz for 90° pulses (corresponding to 90° pulses of 5.0 μs) and the CP. The contact time for the CP process was 5.0 ms. A Hahn echo ($\tau-^{29}$Si π-pulse$-\tau$) with $\tau = 30$ μs was applied before the detection of the free induction decay (FID). The ^{1}H decoupling fields of 40 kHz were applied during the FID detection. The dwell time and pulse delay was 25 μs and 10 s, respectively. The acquisition time was typically 12.8 ms. The measurements were carried out at 23−240 °C. Above 150 °C, we used boiled-off nitrogen gas for all the gas flows to avoid damage to the probe and variable temperature apparatus. The temperatures appearing in this paper were the calibrated by ^{207}Pb measurements.[19] At 240 °C, the CP/CSA spectra were also measured under ultraslow MAS with various rotation frequencies of less than 100 Hz, as indicated below. The acquisition time was extended to 51.2 ms for the ultraslow MAS measurements which provide spinning sideband patterns. Moreover, ^{29}Si direct polarization CSA (DP/CSA) experi-

* To whom correspondence should be addressed. E-mail: kaji@scl.kyoto-u.ac.jp.

10.1021/ma070790y CCC: $37.00
Published on Web 06/20/2007

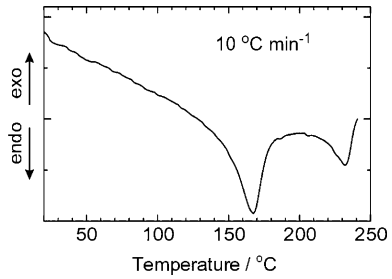

Figure 1. DSC thermogram of poly(dimethylsilane) (PDMS) at the heating rate of 10 °C min^{-1}.

ment without CP preparation was carried out for the static sample at 240 °C. For the excitation, 90° pulse is applied. The pulse delay of 280 s, which was longer than 3 times the ^{29}Si spin−lattice relaxation time (T_{1Si}), was used for this experiment. For the determination of the T_{1Si} value, the CPT1 pulse sequence[20] was used, and the measurement was carried out under MAS conditions. Except for the parameters specified above, all the other experimental parameters for ultraslow MAS and DP/CSA experiments were the same with the CP/CSA experiments. ^{29}Si chemical shifts were expressed as values relative to tetramethylsilane (Me_4Si) by using the CP/MAS single resonance line at −34.0 ppm for PDMS at 23 °C. For the processing of the FID, no broadening functions were applied unless otherwise noted. The measurements were carried out up to 240 °C, which was only 8 °C higher than the higher transition observed by DSC. The solid-state NMR measurements higher than 240 °C could not be carried out due to the limitation of our solid-state NMR hardware.

Differential scanning calorimetry (DSC) measurements were performed on a TA Instruments DSC 2910 differential scanning calorimeter at a heating rate of 10 °C min^{-1}. Indium was used as the standard for the temperature calibration. All the DSC measurements were carried out under flowing N_2 gas.

Results and Discussion

DSC Experiments. Figure 1 shows the DSC thermogram of PDMS. Two endothermic peaks were observed at 166 and 232 °C with the ΔH of 0.5−0.8 and 0.2 J mol^{-1}, respectively. This agrees with previous reports.[17,18] The ΔH value for the transition at the lower temperature depends on how the baseline is estimated.

^{29}Si CP/CSA Experiments. Figure 2 shows the ^{29}Si CP/CSA spectra of PDMS. Sample spinning is not applied in this case, and all the spectra in this figure are measured for the static sample. Below the lower transition temperature of 166 °C, we can observe typical CSA line shapes; the peak and shoulders, which correspond to the chemical shift principal values of σ_{11}, σ_{22}, and σ_{33}, are observed as shown by the vertical broken lines in this figure, although the separation of σ_{22} and σ_{33} is not very obvious. We simulated the experimental CSA spectrum at 23 °C. The simulated CSA spectrum, shown on the experimental CSA spectrum at 23 °C by a thick broken curve, agrees well with the experimental spectrum. The principal values, σ_{11}, σ_{22}, and σ_{33}, are determined to be −15.0, −43.0, and −46.0 ppm, respectively, from the simulation.

Magic Angle Hole in ^{29}Si CP/CSA. Above the transition temperature of 166 °C, the observed CSA line shapes are found to be different from the typical CSA line shapes. The intensity near the center of gravity, namely the isotropic chemical shift (∼34 ppm), becomes small compared to the typical CSA line shapes, as shown in Figure 2e−h. We assume that this "hole" results from the uniaxial rotational motion of the PDMS chains. Under the uniaxial rotation, the ^{1}H−^{29}Si dipolar interaction averages to be parallel to the direction of the rotation axis. The ^{1}H−^{29}Si dipolar vector is then always directed to the polymer

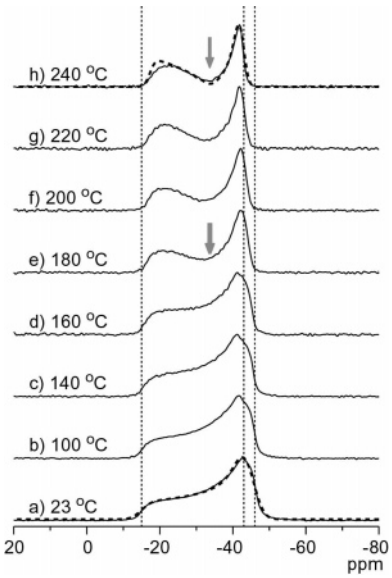

Figure 2. Temperature dependence of ^{29}Si CP/CSA spectra of PDMS from 23 to 240 °C. The chemical shift principal values, σ_{11}, σ_{22}, and σ_{33}, are indicated by the broken vertical bars. The arrow indicates the isotropic chemical shift, that is, the theoretical position of the magic angle hole. The simulated spectra for the experimental spectra of 23 and 240 °C are shown by the thick broken curves.

chain axis. The dipolar coupling under the static magnetic field, $\mathbf{B}_0$, is described as

$$\omega_{SiH} = \frac{\gamma_{Si}\gamma_H}{r^3}\frac{1}{2}(3\cos^2\theta - 1) \qquad (1)$$

where θ is the angle between the ^{1}H−^{29}Si dipolar vector and $\mathbf{B}_0$. Therefore, the ^{1}H−^{29}Si dipolar coupling becomes zero for the chains directed to the magic angle, 54.7°, relative the $\mathbf{B}_0$ ($(3\cos^2 54.7° - 1)/2 = 0$). During the CP process, the magnetization transfer from ^{1}H to ^{29}Si occurs via the ^{1}H−^{29}Si dipolar coupling, resulting in the zero intensity at the isotropic chemical shift of the CP/CSA spectra. The intensities for the polymer chains directed near the magic angle are also attenuated according to eq 1. A more detailed theoretical background was provided in ref 21, and this concept was applied to the uniaxially rotated samples in refs 21−24. According to refs 23 and 24, we call the hole the "magic angle hole". The simulated spectrum, taking the effect of the magic angle hole into account, is shown on the experimental spectrum in Figure 2h. This simulation well reproduces the experimental spectrum at 240 °C. The motionally averaged principal values, $\bar{\sigma}_{11}$, $\bar{\sigma}_{22}$, and $\bar{\sigma}_{33}$, were determined to be −17.4, −42.4, and −42.4 ppm, respectively. The CSA line shapes are found to be axially symmetric ($\sigma_{22} = \sigma_{33}$), which additionally confirms the uniaxial chain rotation in the PDMS. The axially symmetric CSA line shapes are more clearly shown below.

^{29}Si DP/CSA Experiment. The simulation of the CP/CSA spectrum at 240 °C shows the intensity attenuation that originated from the concept of magic angle hole. To confirm this, a ^{29}Si DP/CSA spectrum without the CP preparation was measured at 240 °C. The magic angle hole is assumed to have originated from the CP process with the angular dependent ^{1}H−^{29}Si dipolar coupling. Therefore, it is expected that the magic angle hole disappears by using direct ^{29}Si single-pulse excitation without the CP. Figure 3a shows the ^{29}Si DP/CSA spectrum without using the CP process. In contrast to the CP/CSA spectra in Figure 3c, no hole is observed at the isotropic chemical shift. This confirms that the origin of the hole is the disappearance

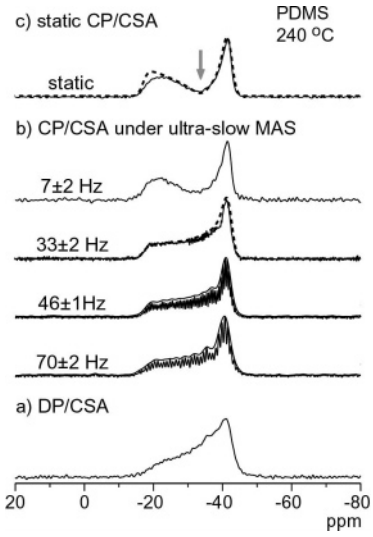

Figure 3. (a) ^{29}Si DP/CSA spectrum of PDMS at 240 °C. (b) CP/CSA spectra of PDMS at 240 °C under ultraslow MAS of 7−70 Hz. The CP/CSA spectrum of PDMS at 240 °C in Figure 2h is also shown for the reference in (c). The simulated spectrum for the experimental spectrum under 33 Hz spinning are shown by the thick broken curves. The envelope curves for the spectra under 46 and 70 Hz spinning are the same experimental spectra, but the 100 Hz Gaussian line broadening function is applied.

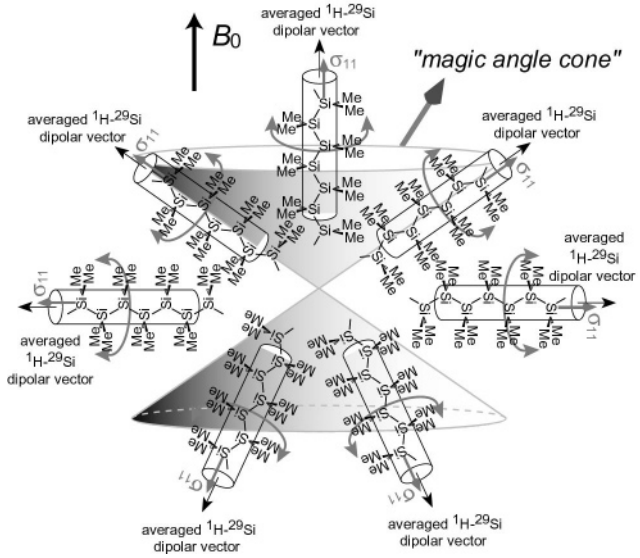

Figure 4. Schematic representation of uniaxial rotational motion of powdered PDMS sample. Under the motion, ^{1}H−^{29}Si dipolar vector is averaged to be parallel to the local chain axis, and therefore the dipolar coupling vanishes for the PDMS chains on the "magic angle cone". Principal shielding orientations for main-chain ^{29}Si of PDMS are also shown; the direction of the σ_{11} direction is well-defined as the local chain axis whereas the directions of σ_{22} and σ_{33} are not well-defined.

of the ^{1}H−^{29}Si dipolar coupling at the magic angle direction during the CP process. However, a long recycle delay of 280 s ($>3T_{1Si}$) was necessary for this measurement due to the long ^{29}Si spin−lattice relaxation even at the high temperature of 240 °C. A long accumulation time of 10 h was needed for this experiment. Moreover, the line shape of Figure 3a is still slightly distorted; the intensity at σ_{11} is low compared for the theoretical line shape. This occurs when materials undergo a uniaxial rotation, because the spin−lattice relaxation becomes anisotropic in such cases. The T_1 value for the rotation axis, which corresponds to the σ_{11} direction in our case, is greater than the T_1 values for the direction perpendicular to the rotation axis (corresponding to the σ_{22} and σ_{33} directions). The anisotropic spin−lattice relaxation was previously observed for the uniaxially rotating solid benzene at −126 °C.[25] In our experiments, the determination of the T_{1Si} value was carried out under the MAS conditions. The obtained T_{1Si} value is therefore the average value of the orientation-dependent T_{1Si} values, and T_{1Si} for the σ_{11} component would be longer. A much longer recycle delay would then be necessary to obtain the fully relaxed CSA spectrum. The experiment is much more time-consuming. Here, we only would like to obtain the result of vanishing the magic angle hole without using the CP process. The present experimental spectrum confirms the anticipated behavior.

^{29}Si CP/CSA Experiments under Ultraslow MAS. The DP/CSA experiment shows that the modulated spectral patterns are due to the angular dependence of the ^{1}H−^{29}Si dipolar interaction during the CP process. However, a long experimental time is needed to obtain the fully relaxed theoretical CSA spectrum. Here, we demonstrate an alternative, less time-consuming, and simpler method to confirm the concept of the magic angle hole and to retrieve the typical CSA spectra. Figure 3b shows the CP/CSA spectra under ultraslow MAS conditions with the spinning rate of 7−70 Hz. The static CSA spectrum is also shown for comparison in Figure 3c. At the spinning speed of 7 Hz, the spectral pattern is almost the same as the static CSA pattern, and the magic angle hole is clearly observed. However, at the spinning speed of 33 Hz, a standard axially symmetric CSA pattern is observed and the magic angle hole disappears. The reason for the disappearance of the magic angle hole is shown in Figure 4. Without the MAS condition, the uniaxially rotating PDMS chains on the "magic angle cone" in this figure produce a zero dipolar coupling, because the averaged ^{1}H−^{29}Si dipolar interaction, directed to the local chain axis, is along the magic angle relative to $\mathbf{B}_0$. Under the ultraslow MAS condition, all the PDMS chains artificially rotate around the MAS rotation axis. The PDMS chains on the magic angle cone under the static condition are no longer on the magic angle cone. The exception is only the few chains along the MAS rotation direction. The effect is therefore negligibly small. Therefore, the ultraslow MAS retrieves the ^{1}H−^{29}Si dipolar coupling even for the PDMS chains on the magic angle cone in the static state. The magic angle hole then disappears by applying the ultraslow MAS, and typical axially symmetric CSA patterns are obtained. At higher spinning speeds (46 and 70 Hz in Figures 3b), the spectra start to split into spinning sidebands. However, the envelopes are axially symmetric CSA patterns without the magic angle hole, as is found from the spectra by applying the 100 Hz Gaussian broadening function (see the envelope curves in Figure 3b). Note that the line widths of the respective sidebands are ∼30−40 Hz and that of the CP/MAS spectrum at 240 °C is 25 Hz. Each of the ultraslow MAS spectra in Figure 3b needs only 10 min for accumulation, which is significantly shorter than the DP/CSA spectrum in Figure 3a. For the spectra in Figure 3b, the spinning speed is stabilized within ±1−2 Hz even at the high temperature. Although stable ultraslow MAS have been accomplished by recent developments,[26−31] the stabilization is sometimes difficult, especially at elevated temperatures. However, the present experiments are aimed only to retrieve typical CSA patterns and do not need such a stable sample rotation.

From an analytical point of view, we present a simple solid-state NMR method to detect the rotational motion in solid materials. The "magic angle hole" in the CP/CSA spectra without sample spinning originates from the rotational motion in the materials, and therefore, the occurrence of the rotational motion can be examined by simply measuring the CSA spectra.

From the DSC curve in Figure 1, another transition is also observed at 232 °C. Our solid-state NMR experiments below and above this transition do not show any significant changes in the CSA line shapes. Further high temperature solid-state NMR experiments would be necessary to characterize the transition. However, this could not be carried out due to the temperature limitation of our NMR system.

Conclusion

The solid-state NMR characterization of the solid−solid transition of PDMS at 166 °C and the mesophase above the transition temperature, which has not been well characterized so far, was carried out by measuring the ^{29}Si CSA line shapes. Below the transition temperature, typical CP/CSA spectra are obtained. In contrast, the intensity "holes" are observed at the isotropic chemical shift of the CP/CSA powder patterns above the transition temperature. The hole, termed "magic angle hole", in the CSA spectra represent clear experimental evidence that the PDMS chains undergo a uniaxial rotation motion along the chain axis in the mesophase. For polymer chains under uniaxial rotations, the dipolar interaction between ^{1}H and a nucleus under observation is averaged to become parallel to the rotation axis. The angular dependence of the dipolar interaction is described by the second-order Legendre polynomial, P_2. Therefore, the signal intensity attenuation occurs during the CP process for polymers whose rotation axis is oriented near along the magic angle relative to the applied magnetic field, $\mathbf{B}_0$. The theoretical simulation considering the orientation dependence of the CP efficiency successfully explains the experimental spectrum with the magic angle hole. The concept of the magic angle hole is confirmed by the ^{29}Si DP/CSA and ultraslow MAS CP/CSA experiments, which retrieve the normal CSA spectrum without the magic angle hole. The axially symmetric CSA patterns are obtained in these experiments. These are additional experimental evidence that the PDMS is in the rotator phase above 166 °C. The change in the interchain packing from a monoclinic to a hexagonal lattice observed by Lovinger et al. therefore originates from the chain rotation dynamics around the molecular chain axis.

Acknowledgment. H.K. thanks Dr. C. S. Yannoni for his useful advice and Prof. Mei Hong for her publications on the magic angle hole. This work was partially supported by a Grant-in-Aid for Scientific Research (A) (No. 17205018) from the Ministry of Education, Culture, Sports, Science and Technology (MEXT), Japan.

References and Notes

(1) Wunderlich, B.; Moller, M.; Grebowicz, J.; Baur, H. *Adv. Polym. Sci.* **1988**, *87*, 1.
(2) Ungar, G. *Polymer* **1993**, *34*, 2050.
(3) Auriemma, F.; De Rosa, C.; Corradini, P. *Adv. Polym. Sci.* **2005**, *181*, 1.
(4) Ungar, G.; Stejny, J.; Keller, A.; Bidd, I.; Whiting, M. C. *Science* **1985**, *229*, 386.
(5) Vaughan, A. S.; Ungar, G.; Bassett, D. C.; Keller, A. *Polymer* **1985**, *26*, 726.
(6) Ungar, G. *Macromolecules* **1986**, *19*, 1317.
(7) Sirota, E. B.; King, H. E.; Shao, H. H.; Singer, D. M. *J. Phys. Chem.* **1995**, *99*, 798.
(8) Sirota, E. B.; Herhold, A. B. *Polymer* **2000**, *41*, 8781.
(9) Becker, J.; Comotti, A.; Simonutti, R.; Sozzani, P.; Saalwachter, K. *J. Phys. Chem. B* **2005**, *109*, 23285.
(10) Sawai, D.; Kanamoto, T.; Porter, R. S. *Macromolecules* **1998**, *31*, 2010.
(11) Hu, W. G.; Boeffel, C.; Schmidt-Rohr, K. *Macromolecules* **1999**, *32*, 1611.
(12) Hu, W. G.; Schmidt-Rohr, K. *Acta Polym.* **1999**, *50*, 271.
(13) Nakae, M.; Uehara, H.; Kanamoto, T.; Zachariades, A. E.; Porter, R. S. *Macromolecules* **2000**, *33*, 2632.
(14) Kaji, H.; Miura, N.; Schmidt-Rohr, K. *Macromolecules* **2003**, *36*, 6100.
(15) Sawai, D.; Kanamoto, T.; Yamazaki, H.; Hisatani, K. *Macromolecules* **2004**, *37*, 2839.
(16) deAzevedo, E. R.; Bonagamba, T. J.; Reichert, D. *Prog. Nucl. Magn. Reson. Spectrosc.* **2005**, *47*, 137.
(17) Lovinger, A. J.; Davis, D. D.; Schilling, F. C.; Padden, F. J.; Bovey, F. A.; Zeigler, J. M. *Macromolecules* **1991**, *24*, 132.
(18) Varma-Nair, M.; Cheng, J. L.; Jin, Y. M.; Wunderlich, B. *Macromolecules* **1991**, *24*, 5442.
(19) Bielecki, A.; Burum, D. P. *J. Magn. Reson. A* **1995**, *116*, 215.
(20) Torchia, D. A. *J. Magn. Reson.* **1978**, *30*, 613.
(21) Pines, A.; Gibby, M. G.; Waugh, J. S. *J. Chem. Phys.* **1973**, *59*, 569.
(22) Litvinov, V. M.; Whittaker, A. K.; Hagemeyer, A.; Spiess, H. W. *Colloid Polym. Sci.* **1989**, *267*, 681.
(23) Yamaguchi, S.; Huster, D.; Waring, A.; Lehrer, R. I.; Kearney, W.; Tack, B. F.; Hong, M. *Biophys. J.* **2001**, *81*, 2203.
(24) Hong, M.; Doherty, T. *Chem. Phys. Lett.* **2006**, *432*, 296.
(25) Gibby, M. G.; Waugh, J. S.; Pines, A. *Chem. Phys. Lett.* **1972**, *16*, 296.
(26) Gan, Z. H. *J. Am. Chem. Soc.* **1992**, *114*, 8307.
(27) Hu, J. Z.; Orendt, A. M.; Alderman, D. W.; Pugmire, R. J.; Ye, C. H.; Grant, D. M. *Solid State Nucl. Magn. Reson.* **1994**, *3*, 181.
(28) Hu, J. Z.; Wang, W.; Liu, F.; Solum, M. S.; Alderman, D. W.; Pugmire, R. J.; Grant, D. M. *J. Magn. Reson. A* **1995**, *113*, 210.
(29) Kaji, H.; Horii, F. *J. Chem. Phys.* **1998**, *109*, 4651.
(30) Hu, J. Z.; Wang, W.; Bai, S.; Pugmire, R. J.; Taylor, C. M. V.; Grant, D. M. *Macromolecules* **2000**, *33*, 3359.
(31) Kaji, H.; Fuke, K.; Horii, F. *Macromolecules* **2003**, *36*, 4414.

MA070790Y